MECHANICAL PROPERTIES OF

CONTROLLED GRAIN STRUCTURE (CGS) ALLOY 718

D. A. Chang, R. Nasser-Rafi, and S. L. Robertson

Technical Center
Structurals Division
Precision Castparts Corp.
4600 SE Harney Drive
Portland, Oregon 97206-0898

Abstract

Controlled Grain Structure (CGS) technology for investment castings is capable of producing an equiaxed grain structure (ASTM 3 to 5 micrograin size) in Alloy 718. In contrast, conventional investment casting methods often produce large, columnar grain structures. The CGS microstructure offers significant improvements in the mechanical properties of cast Alloy 718, especially tensile strengths and low cycle fatigue life. Gas tungsten arc welding (GTAW) of CGS Alloy 718 did not have a detrimental effect upon the properties measured in this study except for the low cycle fatigue life at 538°C (1000°F) and ductility at 649°C (1200°F) for the heat treatment employed. Even then, the LCF lives of welded, CGS Alloy 718 specimens exceeded the lives of their non-welded, conventionally cast counterparts. Fractographic analysis showed that failure preferentially occurred in the base metal or heat-affected zone (HAZ), but not in the weld metal, for both conventionally cast and CGS Alloy 718.

Superalloys 718, 625 and Various Derivatives
Edited by Edward A. Loria
The Minerals, Metals & Materials Society, 1991

Introduction

Why CGS Technology?

Design criteria for aerospace structural castings are more demanding than ever before. In particular, increased low cycle fatigue and tensile properties are needed for gas turbine applications presently using Alloy 718. Continuing demands for increased fuel efficiency through weight reduction and for reduced maintenance costs through greater cast product reliability require improvements in these mechanical properties.

Controlled Grain Structure (CGS) technology is being developed at PCC to meet these needs. Although the term CGS denotes products with a finer grain structure than conventional investment castings, its emphasis is on achieving microstructures which give the mechanical properties our customers desire. PCC has a number of techniques to produce a range of refined microstructures.

This paper presents the findings from a study which initiated a database for CGS Alloy 718. Selected mechanical properties of CGS Alloy 718 are compared with those of conventionally cast Alloy 718. In addition, the effect of gas tungsten arc welding on the microstructure and mechanical properties of both types of Alloy 718 is discussed.

Test Material and Heat Treatments

Test material was cast from Alloy 718 of the composition listed in Table I.

Table I. Composition of Alloy 718 Test Material

Element	Weight Percent	Element	Weight Percent
Ni	52.77	C	0.06
Cr	17.86	Mn	0.03
Nb	5.10	Cu	0.02
Mo	3.09	Ta	0.02
Ti	0.86	Zr	0.01
Al	0.47	P	0.008
Si	0.16	S	0.005
Co	0.11	B	0.003
Fe	balance		

The test specimens were predominantly comprised of cast-to-size (CTS) bars and bars excised from 19 mm (0.75 inch) square blanks. As shown in Figure 1A, the CTS and excised bars were paired to provide a direct mechanical property comparison. These pairs were derived from test bar clusters and were designated as "separately-cast" material to distinguish them from production castings. To facilitate later discussion, the excised bars are called *pseudo* -MFC specimens, where "MFC" refers to "machined-from-casting". The test bar clusters were produced using the conventional investment casting technique and one of PCC's CGS methods.

Some pseudo-MFC test material, representative of both the conventional and CGS casting methods, was welded after hot isostatic pressing (HIP) using a proprietary procedure for gas tungsten arc welding (GTAW). These welds were centered in the gage section. Pseudo-MFC specimens were subsequently machined from the welded blanks.

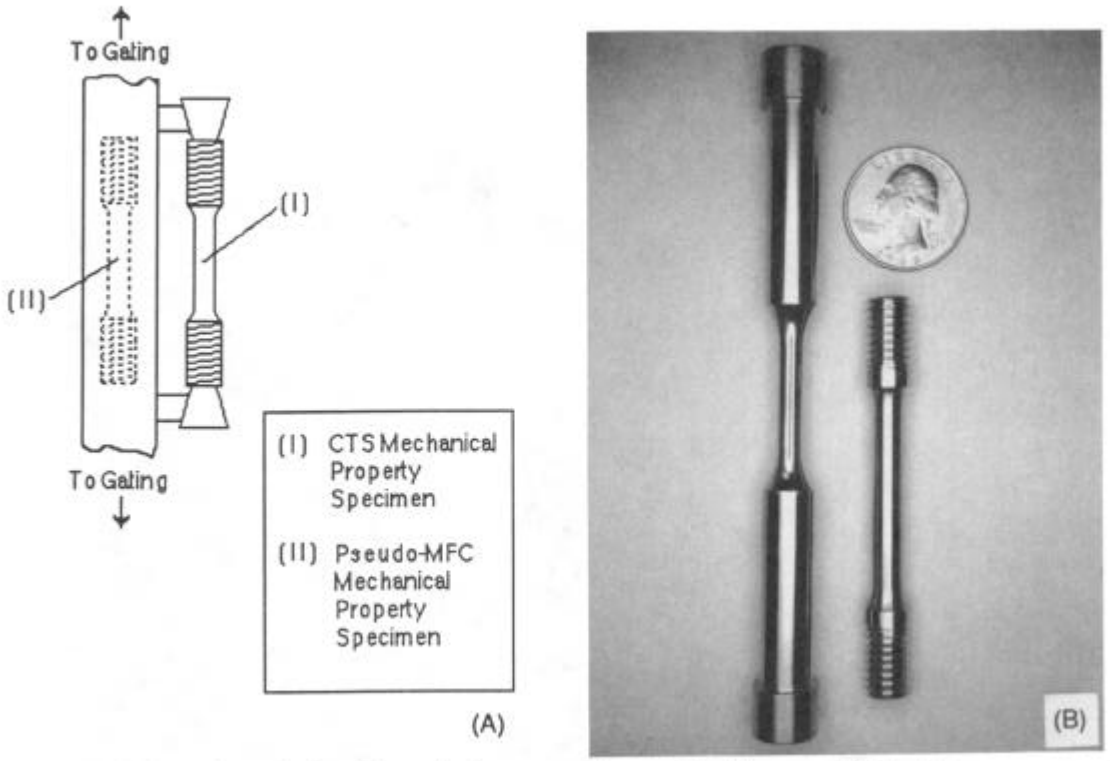

Figure 1. (A) Location of sites for paired, separately-cast test bars. (B) Test bars prepared for low cycle fatigue tests (left) and room/elevated temperature tensile tests (right).

In addition, a lesser number of test bars (MFC) were excised from experimental parts cast by this CGS method. None of these test bars were welded. The portion of the castings from which these were taken had a section thickness of approximately 16 mm (0.625 inch).

Most of the test material was given the same thermal treatment, according to a customer-proprietary schedule (Heat Treatment A), which included separate homogenization, HIP, solutioning, and aging steps. The material was allocated to permit statistical comparison between sample groups for the following tests: room temperature tensile, 649°C (1200°F) tensile, 649°C (1200°F) notched stress-rupture, and 538°C (1000°F) low cycle fatigue. Figure 1B shows examples of the machined test bars. A limited number of specimens were given a new, proprietary heat treatment (Heat Treatment B).

Microstructures

Conventional and CGS Microstructures

Typical microstructures after HIP for conventionally cast and CGS Alloy 718 are presented in Figures 2A and 2B. Because the CGS Alloy 718 material had an equiaxed grain structure, the micrograin size after each stage of Heat Treatment A was measured using the linear intercept method of ASTM E-112.[i] Metallographic preparation involved electrolytically etching each specimen at 3.5V with a 10% oxalic acid - deionized water solution. As shown in Table II, the average grain size of CGS Alloy 718 did not change significantly during heat treatment. Each

[i] The micrograin size of conventionally cast material was not measured because it is non-equiaxed by nature.

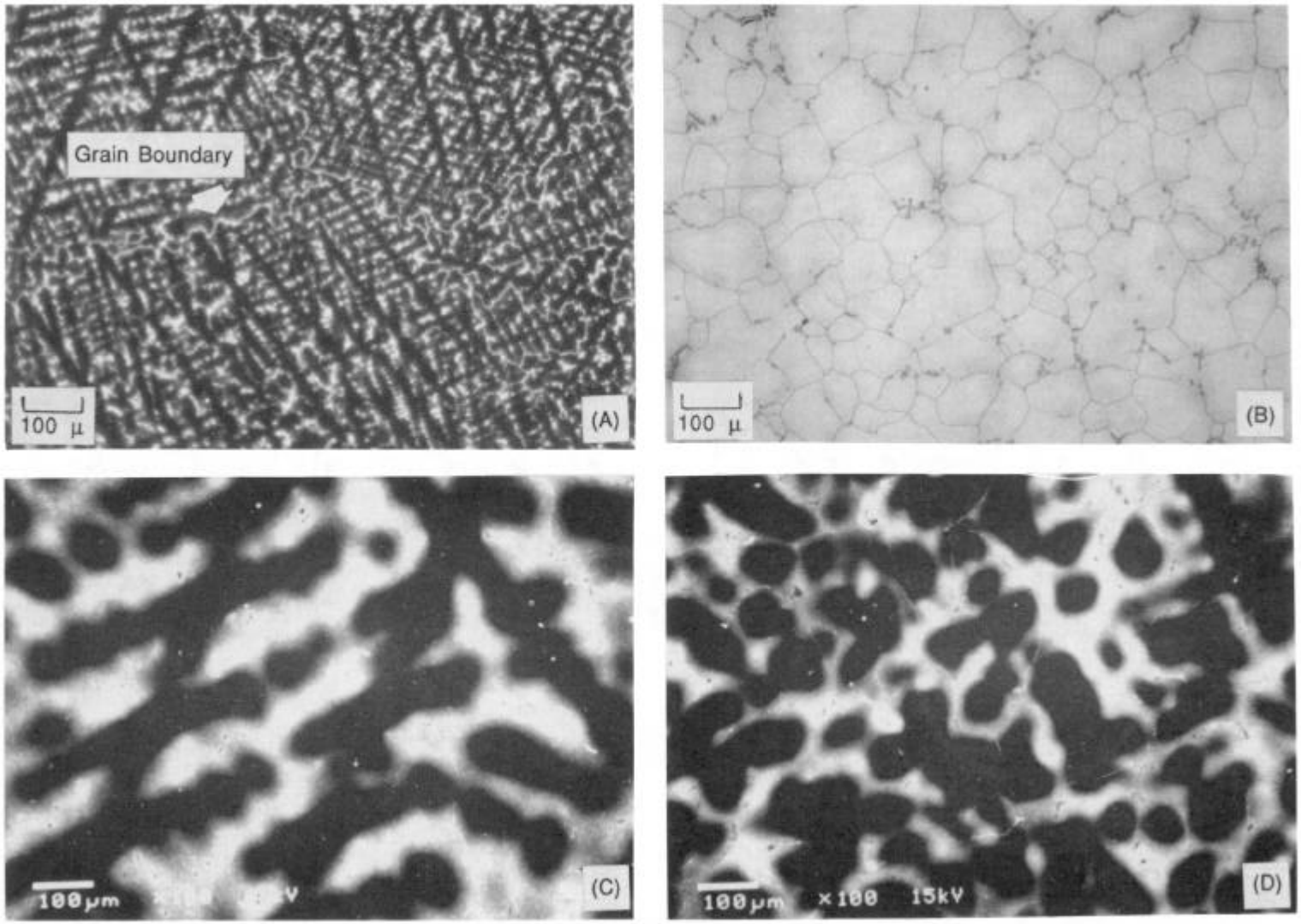

Figure 2: Optical photomicrographs of (A) conventionally cast (darkfield) and (B) CGS Alloy 718 (brightfield) in the HIPed condition. Microsegregation patterns for Nb in (C) conventionally cast and (D) CGS Alloy 718.

Table II. Results of Grain Size Metallography for CGS Alloy 718 in the Homogenized and Fully Heat Treated Conditions (Heat Treatment A)

Source	Heat Treat Condition: Homogenized		Fully Heat Treated	
	ASTM Grain Size	Nominal Grain Diameter (μm)	ASTM Grain Size	Nominal Grain Diameter (μm)
Part	3.9 ± 0.1	84 ± 3	4.2 ± 0.1	76 ± 3
Test Bar Cluster	4.1 ± 0.1	78 ± 2	4.2 ±0.1	75 ± 3
	(95-percent confidence intervals)			

source of test material exhibited slight grain size variations depending on section thickness. This difference was noted for material in the homogenized condition.

The SEM photomicrographs in Figures 2C and 2D respectively show conventionally cast and CGS Alloy 718 given the tag heat treatment described by Corrado et al. (1) which enhances the contrast between regions of high and low Nb content. The microsegregation patterns differ in their relationship to the grain structure. Whereas for conventionally cast Alloy 718 the Nb-rich regions are interdendritic and inside the grains, the CGS material has these regions restricted to the grain boundaries. Although the secondary arms are not fully formed, the CGS Alloy 718 microstructure also exhibits a dendritic nature. This microstructural effect is related to casting conditions which foster copious, heterogeneous nucleation and mutual competition during solidification.

Welded Microstructures

Figures 3A and 3B show the respective microstructures of the weld metal, heat-affected zone (HAZ), and adjacent base metal for conventionally cast and CGS Alloy 718 specimens. In either case, the weld metal microstructure was much finer than the base metal microstructure.

Mechanical Properties

The mechanical property data derived from the sample groups were statistically evaluated using analysis of variance (ANOVA) techniques to determine whether the groups were discernible. The following sections focus on the results for the separately-cast material (CTS and pseudo-MFC), and compare them to results for specimens excised from parts (MFC). Mechanical property data are presented in bar graphs. The differences which are shown in these graphs and discussed below were statistically significant. Except where noted, the results presented below are restricted to Heat Treatment A.

Tensile Properties

The specimens for room temperature and elevated temperature tensile tests were identical. They had gage diameters of 6 mm (0.25 inch) and gage lengths of 25 mm (1.000 inch). Figures 4 and 5 show the tensile properties for the various sample groups at room temperature and 649°C (1200°F), respectively. Data for specimens excised from parts are also included for comparison.

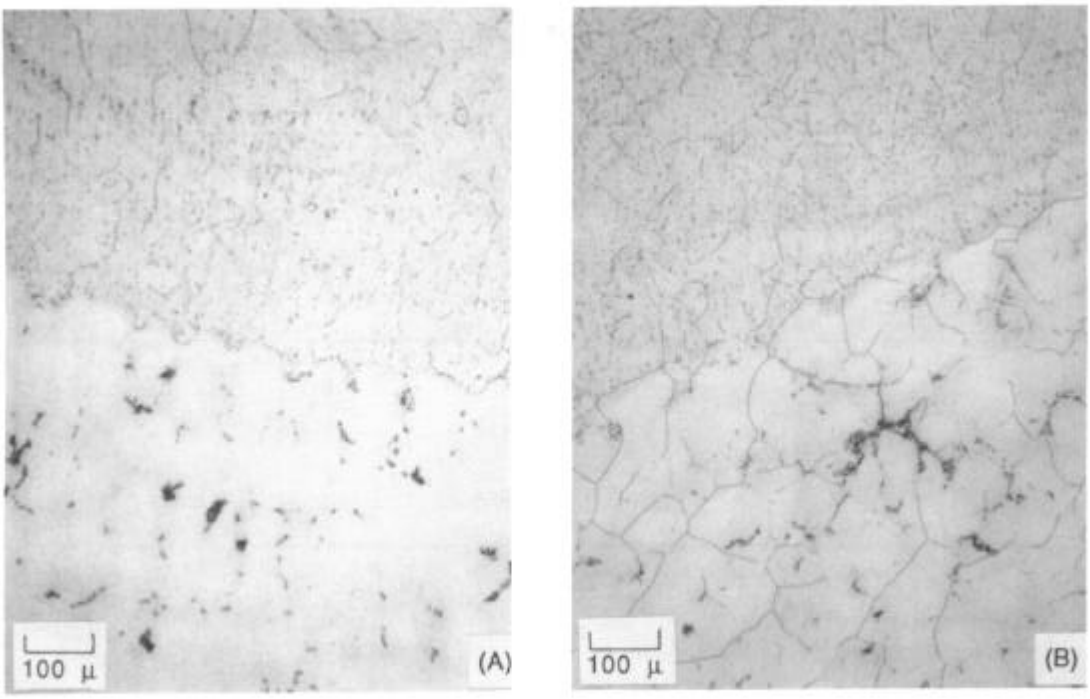

Figure 3. Microstructures adjacent to welds for (A) conventionally cast and (B) CGS Alloy 718. The finer microstructure of the weld deposit can be seen in the top of each photograph.

Room Temperature Tensile Properties. Compared to the conventionally cast Alloy 718 specimens, the CGS material had superior strength, but suffered a concomitant decrease in ductility. The exception to this trend in ductility was observed for the CTS specimens. Figures 4A and 4B compare the ultimate tensile strength and 0.2% offset yield strength for the non-welded specimens, and Figures 4C and 4D show the respective values for percent elongation and percent reduction of area.

An increase in section size caused a consistent decrease in both yield and ultimate tensile strengths for CGS and conventionally cast Alloy 718, but caused different trends in room temperature tensile ductility. The CGS pseudo-MFC specimens were not as ductile as their corresponding CTS specimens. In contrast, the conventionally cast, pseudo-MFC specimens had ductilities equivalent to their corresponding CTS specimens.

The room temperature tensile properties of welded CGS specimens either matched or exceeded the properties of their non-welded counterparts. On the other hand, the ultimate tensile strength and percent elongation of conventionally cast, welded specimens fell below the non-welded specimen measurements.

Figure 4 also compares the properties for CGS pseudo-MFC material with CGS MFC material. No significant difference was found for the yield and ultimate tensile strengths between these sample groups, but the percent elongation and percent reduction of area for pseudo-MFC material were less than for MFC material.

649°C (1200°F) Tensile Properties. In general, the CGS Alloy 718 specimens had higher yield and ultimate tensile strengths, but lower percent elongation and reduction of area than conventionally cast Alloy 718 (Figure 5). As an exception, no significant difference was observed for the percent elongation between the cast-to-size specimens of both casting techniques.

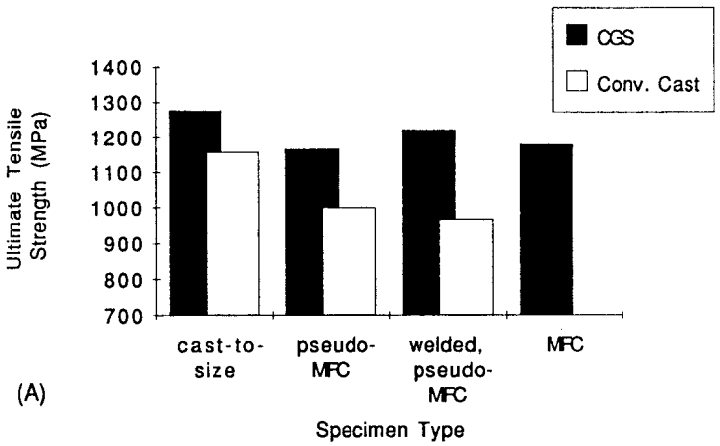

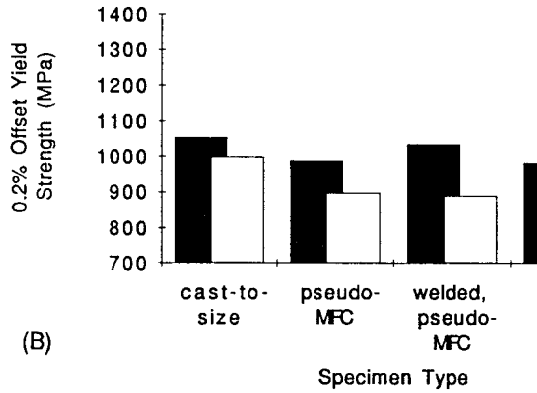

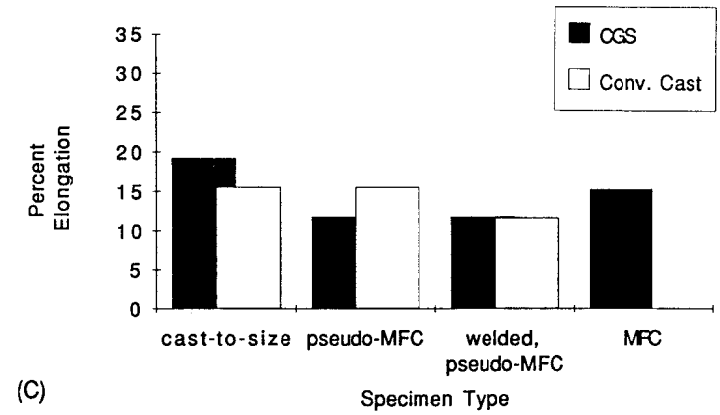

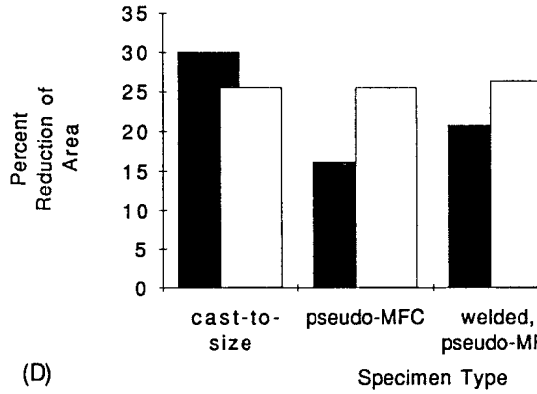

Figure 4: Room temperature tensile properties for Alloy 718 given Heat Treatment A: (A) ultimate tensile streng 0.2% offset yield strength; (C) percent elongation; (D) percent reduction of area. Differences no statistically discernible.

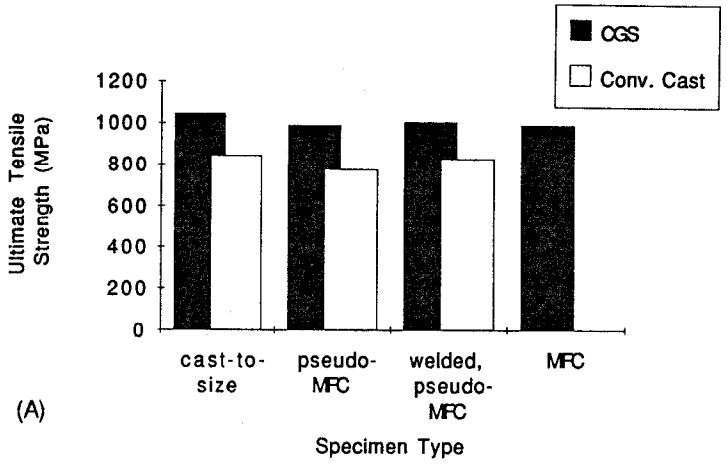

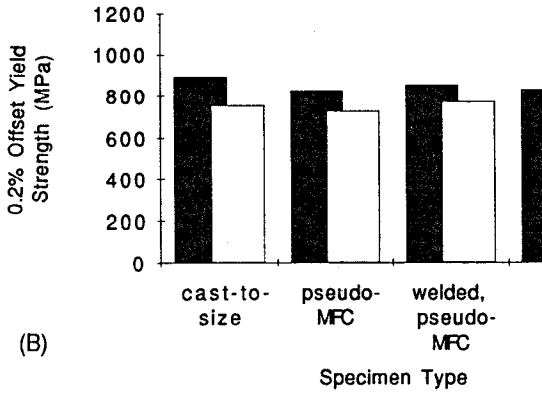

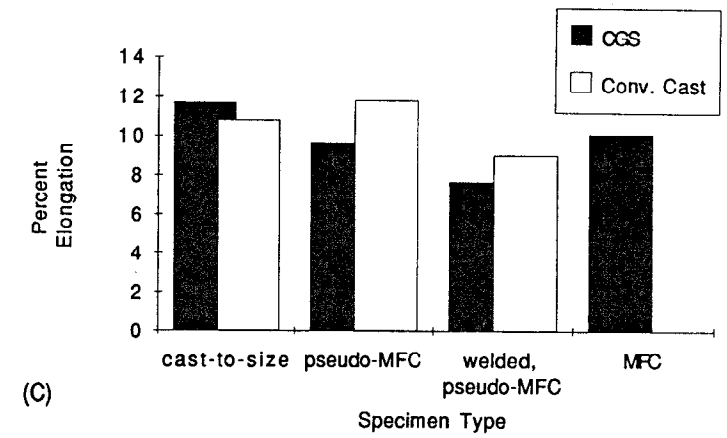

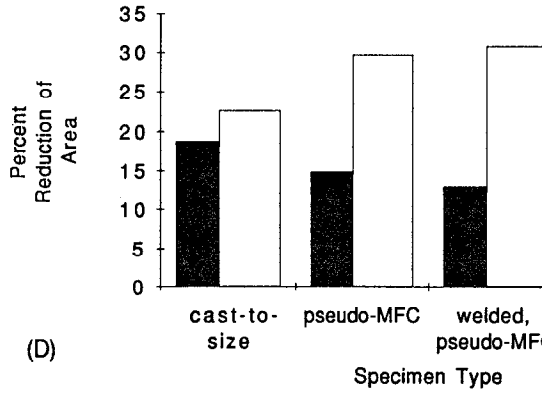

Figure 5: Elevated temperature (649°C, 1200°F) tensile properties for Alloy 718 given Heat Treatment A: (A) u tensile strength ; (B) 0.2% offset yield strength; (C) percent elongation; (D) percent reduction of Differences noted are statistically discernible except for the following comparisons within the percent elor chart: (i) CGS versus conventionally cast in CTS specimens; (ii) CTS versus pseudo-MFC in conventional specimens; and (iii) pseudo-MFC versus MFC in CGS specimens.

Effects relating to section size also were observed for the tensile properties at 649°C (1200°F). The difference in behavior between CGS and conventionally cast Alloy 718 paralleled the results for room temperature tensile properties except for percent reduction of area: the conventionally cast, pseudo-MFC specimens had greater percent reduction of area than the CTS specimens.

Results for welded specimens were typically as good as, or better than, the non-welded specimens. Whether CGS or conventionally cast Alloy 718, the percent elongation was slightly less for the welded specimens at this test temperature.

Figure 5 also compares the pseudo-MFC properties with MFC properties. No significant difference was found in the strength and ductility measurements.

Low Cycle Fatigue

Axial low cycle fatigue (LCF) tests were conducted at 538°C (1000°F) under longitudinal strain control[ii] at 345 MPa (50 ksi) pseudostress. The frequency was 0.5 Hz, using a triangular waveform, and A_e = 1.0. Specimen gage diameter and length were 5 mm (0.200 inch) and 19 mm (0.750 inch), respectively.

Figure 6 shows the LCF lives of welded and non-welded Alloy 718 produced by either conventional or CGS casting methods and given Heat Treatment A. This figure also includes data from a limited number of specimens given Heat Treatment B. The latter results will be addressed in the discussion.

Among the non-welded specimens, the CGS Alloy 718 had a significantly longer life than the conventionally cast material. In addition, the pseudo-MFC specimens exhibited longer LCF lives than their complementary cast-to-size specimens. The longest LCF lives measured in this study were from MFC specimens. Based on this sampling, increased section size exerts a positive influence on the resultant LCF properties.

For both CGS and conventionally cast Alloy 718, welded specimens had shorter LCF lives in comparison to non-welded specimens. Despite the reduction in LCF life caused by welding, the LCF properties of welded CGS specimens were still better than non-welded, conventionally cast pseudo-MFC specimens.

Notched Stress-Rupture

Notched stress-rupture (NSR) testing was conducted using a combination rupture bar. For welded specimens, the notch was machined in the center of the weld. All specimens were tested at 649°C (1200°F) and 621 MPa (90 ksi) using a K_t factor of 2.8. The tests were conducted on a pass-fail basis using a minimum life criterion of 20 hours. Tests were discontinued if they exceeded 300 hours.

Figure 7, which illustrates the fraction of specimens passing the 20-hour minimum life requirement, shows the highest failure rate was measured for CGS Alloy 718 pseudo-MFC specimens given Heat Treatment A. All CTS and welded pseudo-MFC specimens passed the test. This figure also includes data from a limited number of specimens given Heat Treatment B. The latter results will be addressed in the discussion.

Fractographic Analysis

A fractographic analysis was conducted to examine how the non-welded microstructure of investment cast Alloy 718 responded to the various testing conditions, and to determine whether the welds had a detrimental influence. The analytical techniques included optical microscopy for

[ii] Stress controlled after 50,000 cycles.

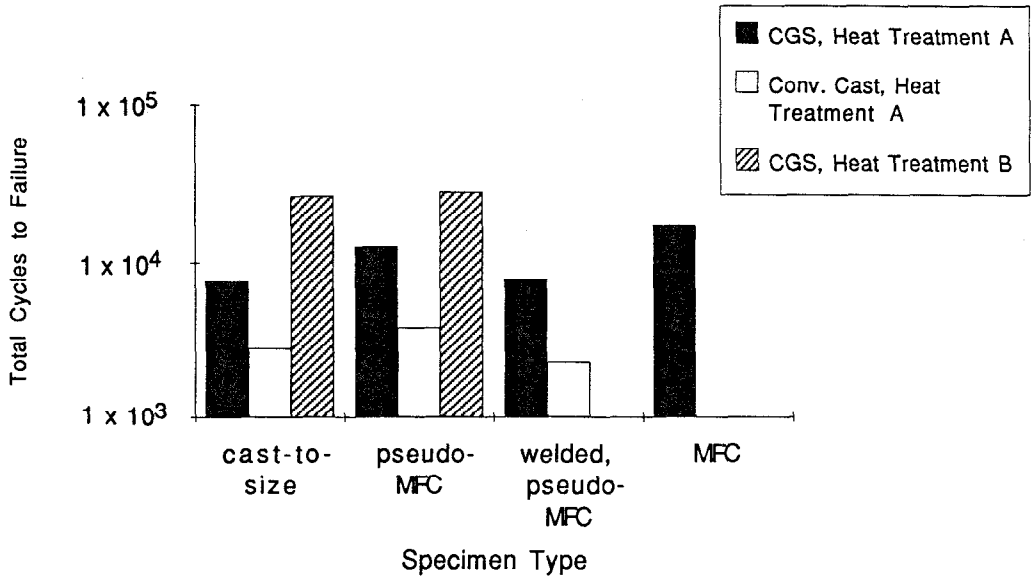

Figure 6. Comparison of low cycle fatigue lives at 538°C (1000°F) for non-welded and welded Alloy 718 cast using conventional and CGS methods. Two additional sample groups are included for comparison: (i) MFC specimens given Heat Treatment A; and (ii) CTS and pseudo-MFC specimens given Heat Treatment B. Differences shown were statistically discernible.

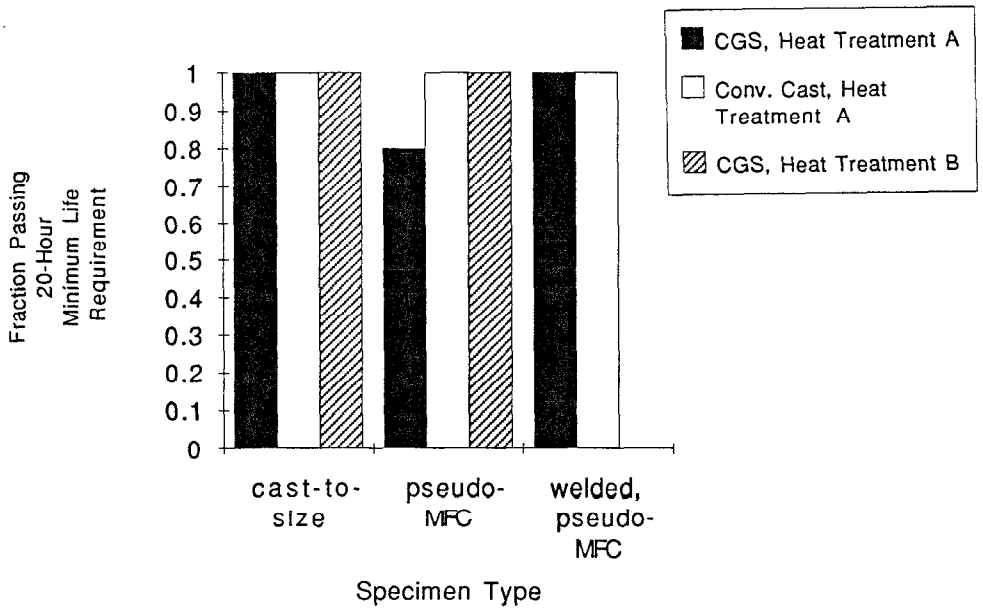

Figure 7. Comparison of notched stress-rupture performance at 649°C (1200°F) for non-welded and welded Alloy 718 cast by conventional and CGS methods. CTS and pseudo-MFC specimens given Heat Treatment B are included for comparison. Differences shown were statistically discernible.

metallographic cross-sections at the site of failure, in conjunction with scanning electron microscopy (SEM) for fracture surface examination.

Non-welded Conventionally Cast and CGS Alloy 718

Primary MC carbide clusters or remnant Laves particles were the principal initiation sites for tensile failure at room temperature and 649°C (1200°F) in both conventionally cast and CGS Alloy 718. Such particles can be seen at the bottom of dimples in the SEM photograph of Figure 8A. Since these phases contain the elements niobium, titanium, and silicon, the distribution of these phases, in parallel with the microsegregation patterns, differed in the two materials

Conventionally cast and CGS Alloy 718 exhibited different fracture behaviors because the location of the primary particles influenced the selection of fracture paths. In CGS Alloy 718, the MC and Laves phases were primarily located along grain boundaries and at grain boundary triple points. Cracks tended to follow grain boundaries as these voids connected. On the other hand, the Laves and MC carbides were mostly in the interdendritic regions of conventionally cast Alloy 718. Therefore, the crack propagated in a transgranular mode when connecting the voids.

Figures 8B, 8C, and 8D illustrate this difference in fracture behaviors. The tensile fracture path of conventionally cast Alloy 718 was transgranular at both ambient and elevated temperature (Figure 8B). In contrast, the fracture path of CGS Alloy 718 depended upon the test temperature. For CGS Alloy 718 tested at room temperature, it was a mixture of intergranular and transgranular propagation (Figure 8C). The fracture path at 649°C (1200°F) was predominantly intergranular in nature (Figure 8D).

The low cycle fatigue specimens typically had initiation sites near the surfaces of the test bars as shown in Figure 9. Normally, crack initiation occurred at areas which appeared quite flat and relatively smooth. Their exact nature has not been determined, but they seem to be associated with crystallographic planes or grain boundaries. In a few cases, initiation occurred at nonmetallic inclusions (aluminum oxides) which reduced the fatigue life of CGS Alloy 718 to a level equivalent to conventionally cast Alloy 718. The SEM micrographs in Figure 9 also show the crack propagation fracture surfaces for these two materials. The CGS Alloy 718 has a rumpled appearance suggesting an intergranular mode at 538°C (1000°F). The conventionally cast material exhibits an interdendritic crack path similar to specimens from other tests.

Effect of Welding

For room temperature tensile, 649°C (1200°F) tensile, and 649°C (1200°F) notched stress-rupture specimens, the failure site was well removed from the weld deposit. This indicated that the welds were stronger than the base metal in all of these tests, regardless of casting method. Representative darkfield optical macrographs are shown in Figure 10. Although the HAZ cannot be clearly distinguished, the fracture site was surmised to be out of the welds' HAZ and actually in the base metal because of the distance involved.

Small welding defects (HAZ microcracks associated with grain boundary liquation and oxides in the fusion zone) were found by metallography in some specimens after testing. (These welding defects fell below the detection capability of radiographic inspection.) Among tensile and NSR specimens, these defects were not associated with the fracture location.

On the other hand, for both CGS and conventionally cast Alloy 718, metallographic examination determined that LCF failures generally occurred near the weld, but not within the weld deposit itself. The proximity to the weld deposit indicated that fracture initiated within the HAZ. In most cases, SEM examination of the fracture surfaces revealed the flat, "crystallographic" type of initiation sites observed for non-welded material. However, other specimens had unusual initiation sites exhibiting such features as the outlines of fine dendrites or smooth, globular surfaces. These latter initiation sites were attributed to HAZ cracks and grain boundary liquation, respectively.

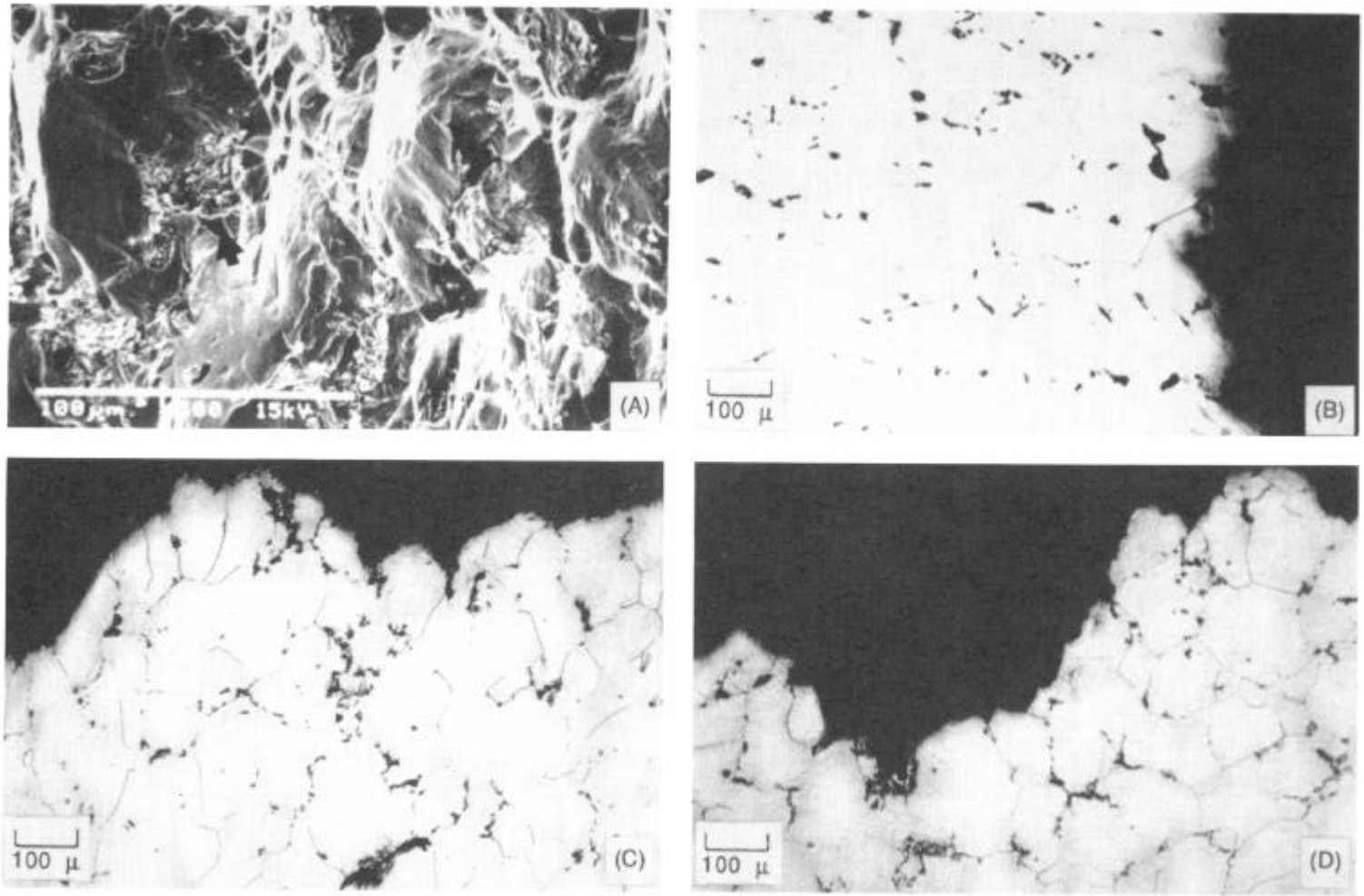

Figure 8: (A) SEM photomicrographs of 649°C (1200°F) tensile specimen fracture surface with Laves and MC carbide particles in dimples. This fracture surface was typical of both CGS and conventionally cast Alloy 718 regardless of test temperature. (B) The tensile fracture path for conventionally cast Alloy 718 was transgranular at both test temperatures. (C) For CGS Alloy 718, at room temperature, the fracture path was a mixture of transgranular and intergranular. (D) At 649°C (1200°F), the fracture path was purely intergranular.

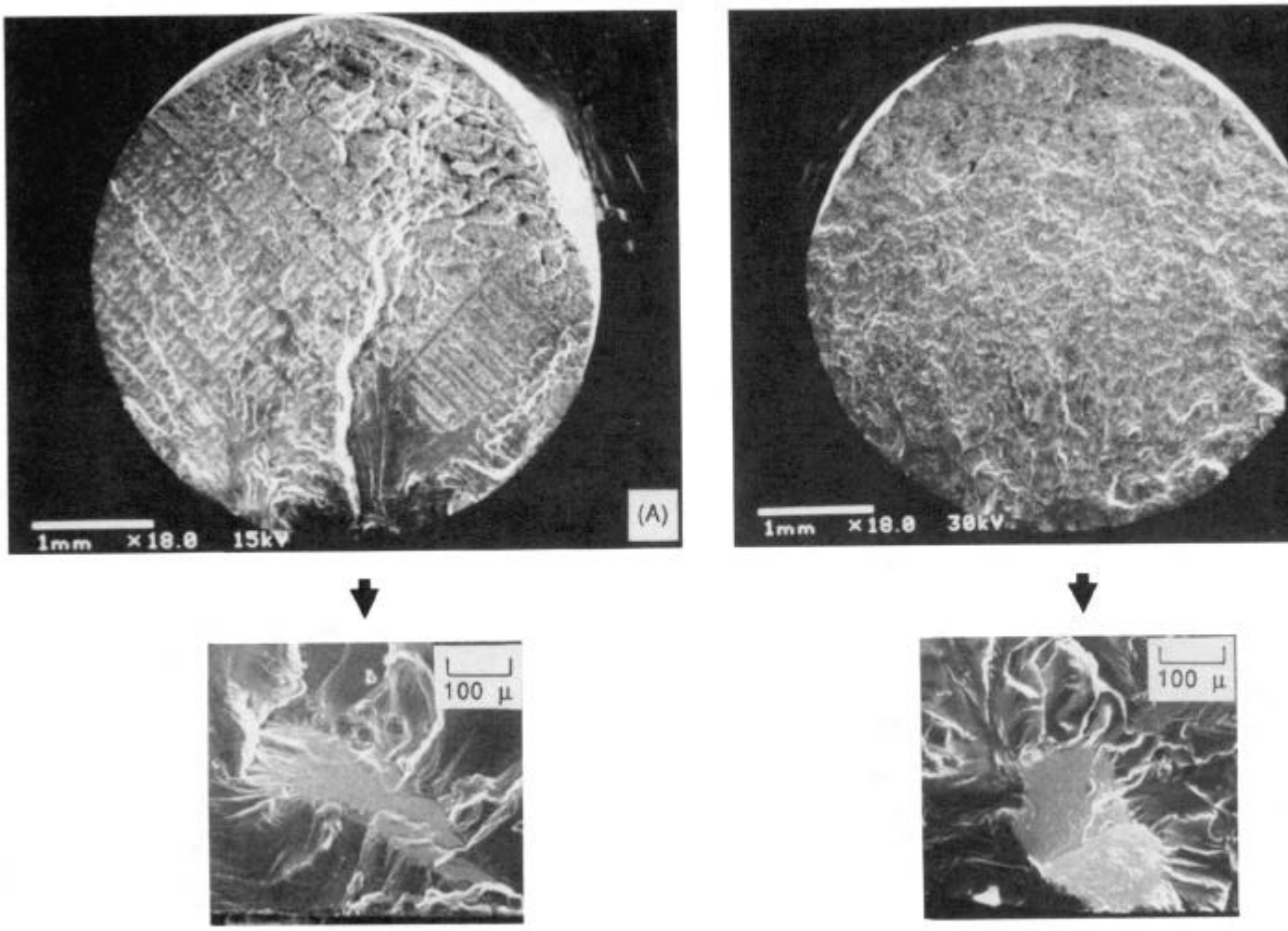

Figure 9: SEM photomicrographs of (A) conventionally cast and (B) CGS Alloy 718 fracture surfaces for specimens low cycle fatigue at 538°C (1000°F). The lower micrographs show the faceted initiation sites near th at higher magnification.

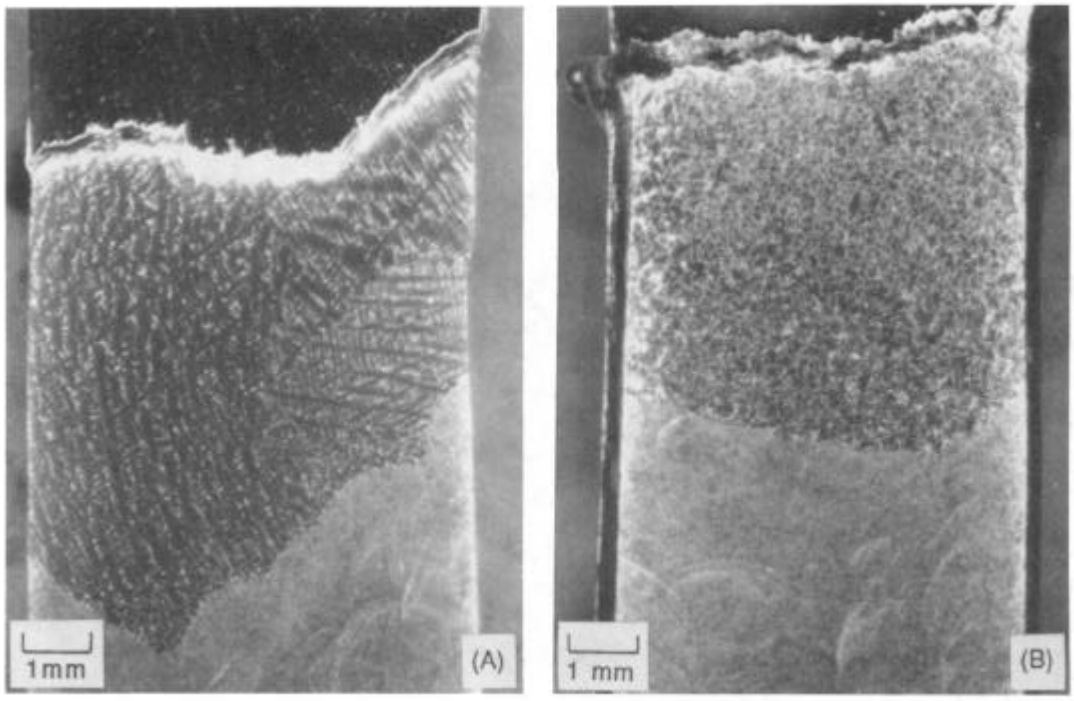

Figure 10. Darkfield optical macrographs showing the failure locations relative to the weld. Failures occurred some distance away from the weld in tensile and notched stress-rupture specimens. (A) Conventionally cast, (B) CGS.

Discussion

Any successful application of CGS Alloy 718 must involve careful consideration of the interchange among mechanical properties and their relationship to the microstructure.

For Alloy 718 given Heat Treatment A, an improvement in low cycle fatigue life is obtainable by application of the CGS process. However, this improvement is hampered by the presence of nonmetallic inclusions. The degree to which LCF life is reduced depends on the size and location of the inclusion as shown in Figure 11. The effect of nonmetallic inclusions on the fatigue life of conventionally cast Alloy 718 could not be predicted from this study.

The trade-off in mechanical properties is emphasized by the tensile and notched stress-rupture results. For Heat Treatment A, the yield strength and ultimate tensile strength are greater for CGS Alloy 718 as compared to conventionally cast Alloy 718, but some decrease in ductility is incurred. The measured decrease was statistically discernible; the engineering significance would depend upon the particular application. CGS Alloy 718 is more notch-sensitive as measured by the NSR test.

The mechanical properties depend on the respective Alloy 718 microstructures. At this time, while the particular mechanisms have not been elucidated, there is sufficient evidence to suggest microstructural alternatives for achieving combinations of mechanical properties. The fractographic analysis indicates that the Laves and MC carbide particles, and thus indirectly the microsegregation patterns, have a role in controlling the ultimate tensile strength and ductility. In addition, the yield strength probably is influenced not only by the grain size and structure because of compatibility and constraint requirements, but also by the microsegregation patterns which influence the relative distribution of strengthening precipitates.

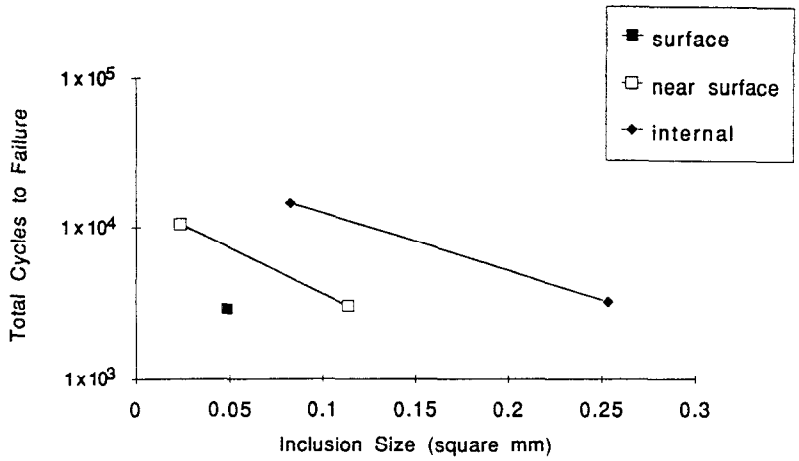

Figure 11. Effect upon the LCF life of inclusion size and location relative to the test specimen's surface. The data represent CGS Alloy 718 given Heat Treatment A.

The difference measured between pseudo-MFC and MFC LCF lives underscores the influence of microstructural characteristics *other than* grain size on mechanical properties. Despite similarities in section thickness and grain size (Table II), the MFC specimens had a longer fatigue life than the pseudo-MFC specimens. This difference further suggests that variables which influence secondary phases also impact mechanical properties.

Aside from influencing the crack propagation path as described earlier, the difference in microsegregation patterns is believed connected to the relative susceptibility to HAZ crack formation. Thompson et al. (2) have related the HAZ cracking in Alloy 718 to the distribution of Laves and MC carbide phases. The LCF life proved to be most sensitive to the presence of welding defects in the HAZ. Despite the reduction in LCF life associated with welding, the LCF life of welded CGS specimens exceeded that of non-welded, conventionally cast pseudo-MFC specimens.

The microstructural evaluation establishes a basis to manipulate the microstructure through alternative heat treatments. Heat Treatment B was applied to improve the notched stress-rupture failure rate for CGS Alloy 718. Although CGS Alloy 718 is notch-sensitive when given Heat Treatment A, Heat Treatment B apparently reduces the notch-sensitivity as shown in Figure 7. An additional advantage, depicted in Figure 6, is an increased LCF life over that of both conventionally cast and CGS Alloy 718 which had been given Heat Treatment A. This occurred with a slight sacrifice in tensile strength, but increased ductility.[iii] The results for Heat Treatment B are encouraging and suggest a possible direction for further study.

Additional work is required for CGS Alloy 718: The mechanical properties of CGS Alloy 718 have not been characterized between room temperature and 538°C (1000°F). Expansion of the mechanical property database temperature range will determine if CGS Alloy 718 given Heat Treatment A is adequate for current design needs.

As more experience is gained with CGS-processed alloys, tailored microstructures within investment castings will come closer to realization.

[iii] Tensile results for Heat Treatment B are not included in this paper.

Conclusions

- The CGS process offers a means to significantly improve the low cycle fatigue life and tensile strengths of investment cast Alloy 718, a result consistent with customer desires. The decrease in percent elongation and percent reduction of area may be mitigated, or even recovered, by alternative heat treatments.

- Nonmetallic inclusions reduce the LCF life of CGS Alloy 718. The magnitude of the effect depends on an inclusion's size and location relative to the surface. The effect of nonmetallic inclusions on the fatigue life of conventionally cast Alloy 718 could not be predicted from this study.

- Microsegregation patterns in CGS Alloy 718 differ from those in conventionally cast Alloy 718. Laves and MC carbides, typically associated with regions of higher Nb content, are the primary initiation sites for tensile failure in either type of Alloy 718.

- CGS Alloy 718 can be successfully welded using proper GTAW techniques.

- The LCF life of both CGS and conventionally cast Alloy 718 is sensitive to the presence of welding defects in the HAZ. However, the LCF life of welded CGS Alloy 718 pseudo-MFC specimens remains superior to those of non-welded, conventionally cast Alloy 718 pseudo-MFC specimens.

- Based on results from non-welded pseudo-MFC specimens, CGS Alloy 718 is more notch-sensitive than conventionally cast Alloy 718. Welded Alloy 718 is not notch sensitive.

- Heat Treatment B offers relief from notch-sensitivity, an extension to LCF life, and better ductility, but with some sacrifice in yield and ultimate tensile strengths.

References

1. J. A. Corrado, W. H. Couts, Jr., and J. F. Radavich, "A Microstructural Test for Chemical Homogeneity in INCONEL 718 Billet," TMS Technical Paper No. A86-34, AIME, Warrendale, Pa., 1986.

2. R. G. Thompson, B. Radhakrishnan, and D. E. Mayo, "Intergranular Liquid Formation, Distribution, and Cracking in the HAZ of Alloy 718 Welds," Superalloy 718 - Metallurgy and Applications, E. A. Loria, ed., TMS, 1989, p. 437.

Acknowledgements

The authors thank Robert Bartocci, Xuan Nguyen-Dinh, and Larry Sink for insightful discussions and editorial comments. Metallographic and SEM services provided by Cris Bellucci, Richard Doty, and Larry Sparks are also appreciated. Stephen Hinote contributed to the welding studies.